INORGANIC CHEMISTRY
FRONTIERS

RESEARCH ARTICLE

View Article Online
View Journal | View Issue

Cite this: *Inorg. Chem. Front.*, 2022, **9**, 3330

Achiral copper clusters helically confined in self-assembled chiral nanotubes emitting circularly polarized phosphorescence†

Ya-Jie Wang,[a] Yan Jin,[a] Xiao-Yan Shi,[a] Xi-Yan Dong *[a,b] and Shuang-Quan Zang *[a]

Received 5th May 2022,
Accepted 24th May 2022

DOI: 10.1039/d2qi00982j

rsc.li/frontiers-inorganic

Integration of atomically precise clusters into chiral nanoassemblies facilitates the fabrication of functional ordered phases with supramolecular chirality, which remains mysterious. Herein, oxygen-sensitive achiral Cu cluster coassembled with a chiral amphiphile to afford helical nanotube, where Cu cluster was confined within the nanotube to emit phosphorescene, and forming helical arrangement with emerged chiroptical activities including circular dichroism (CD) and circularly polarized phosphorescence (CPP), with a relatively large absorptive asymmetry *g*-factor up to 0.018. This work offers a facile and universal protocol for designing chiroptical materials based on coinage metal clusters.

Introduction

Chirality is ubiquitous in nature and closely related to the origin of life. Molecular chirality widely exists in chiral molecules with point, axis and plane types, while ordered aggregation and spatially asymmetric packing achieve advanced chirality transferring from molecular to supramolecular scale, *i.e.*, supramolecular chirality.[1,2] Supramolecular chirality depending on assembly *via* noncovalent forces like electrostatic interaction, H-bonding or aromatic stacking, and those flexible and dynamically manipulated interactions allow for convenient chirality transfer and amplification in the hierarchical assembly.[3,4] During the process of chirality transfer especially homochiral evolution from molecular chirality to supramolecular chirality, the chirality amplification phenomenon appears in the assembled structures.[5] Among the multitudinous assembled structures, helical assemblies usually present significant chirality amplification as the helical configuration providing a chiral environment for the emitters, which dominates the chiroptical properties.[6,7] Moreover, enhanced excitonic coupling and increased active chiral component size as to render the helical assemblies powerful candidates for chirality amplification.[8] In this regard, chemists represented by Liu and Duan have discovered that confining achiral emitters in helical assemblies like chiral nanotubes to realize coassembly is an efficient way to achieve chirality emergence and amplification.[9–14] Compared with the helical assemblies, there are more options for the achiral emitters.

Luminescent atomically precise coinage metal clusters have drawn increasing interests due to their excellent optical properties, which make them as emerging candidates for constructing chiroptical materials.[15,16] Endowing luminescent coinage metal clusters with chirality is a prerequisite for constructing chiroptical materials, the direct strategy is synthesizing chiral coinage metal clusters. However, only few chiral coinage metal clusters with precise atomic structures have been obtained to date.[17–23] The enantioselective synthesis of optically pure chiral coinage metal clusters is still a challenge, as many of them are obtained as racemates which usually should be enantioseparated with low efficiency.[24] However, achiral luminescent clusters are abundant in species.[15] Developing a convenient and universal strategy to endow achiral luminescent clusters with chiroptical properties is conductive to promote the wild application of coinage metal clusters in chiroptical materials. Nowadays, self-assembly is an alternative means to customizing coinage metal clusters for advanced functional materials.[25–30] To this regard, coassembling achiral luminescent clusters with helical soft templates to achieve chirality, even supramolecular chirality, is promising to evolve the chirality properties of achiral clusters, which however have rarely been reported and systematically investigated. We propose that addressing this issue may discover a facile strategy toward chiroptical materials based on achiral coinage metal clusters.

We have reported the chiral assembly of anionic Cu_5^- cluster with chiral amino alcohols by means of cocrystallizing, and the chiral cocrystals achieved impressive circularly polarized phosphorescence (CPP).[31] Nevertheless, the intrinsic

[a]*College of Chemistry, Zhengzhou University, Zhengzhou 450001, China. E-mail: zangsqzg@zzu.edu.cn*
[b]*College of Chemistry and Chemical Engineering, Henan Polytechnic University, Jiaozuo 454000, China*

† Electronic supplementary information (ESI) available. See DOI: https://doi.org/10.1039/d2qi00982j

instability and cultivating difficulty of the cocrystals limited the universality of the chiral cocrystal strategy based on coinage metal clusters. To resolve this issue and develop a facile and universal strategy to endow achiral clusters with chiroptical activities, we carried out a subsequent research based on the above study. By utilizing a pair of protonated chiral glutamic acid derivatives (D/L-G$^+$) as cations, whose neutral molecules are well-demonstrated to form uniform chiral nanotubes during the gelations,[32] we successfully realized chiral coassembly of achiral Cu_5^- cluster and chiral gelator D/L-G$^+$ and inducting the supramolecular chirality and chiroptical activities of Cu_5^- clusters (Scheme 1). Large absorptive asymmetry factor (g_{abs}) up to 0.018 and red CPP emission were obtained from cogel system, in which the chiral gel played an important role for isolating oxygen and as a helical template. A series of experiment results indicated that the well-ordered arrangement of Cu_5^- clusters along the helically chiral nanotubes was crucial for the large optical asymmetry.

Results and discussion

The cogel of Cu_5^- cluster and chiral gelator was obtained directly from cooling the reaction mixture of cuprous oxide, *tert*-butylmercaptan and cations gelator (D/L-G$^+$) under ammonia. To clarify the morphologies of the gels, scanning electron microscopy (SEM) and transmission electron microscopy (TEM) were employed. As shown in Fig. 1a and c, protonated gelator D-G$^+$ formed the helical nanotubes, which is consistent with the neutral gelator.[13,32] After coassembling with Cu_5^- clusters, the regular P-type helical nanotube is retained (Fig. 1b). Under TEM observations, Cu_5^- clusters are well assembled along the chiral nanotubes after cogelation (Fig. 1d and S1†). Furthermore, TEM coupled with energy-dispersive X-ray spectroscopy (TEM-EDS) elemental mapping images confirmed that Cu_5^- clusters were distributed uniformly along the chiral nanotubes. In a strand of nanotube containing Cu_5^- clusters, the elements C, N and O from the chiral gelators are evenly distributed over the whole nanotube, while the elements Cu and S belonging to Cu_5^- clusters are mainly distributed inside the nanotube cavity, confirming that the Cu_5^- clusters are perfectly confined within the core of nanotube (Fig. 1e–h and S2†).

As our previously reported,[31] Cu_5^- cluster is non-emissive in solution as the phosphorescent emission is easily quenched by oxygen. Under UV irradiation, the cogel displays bright red emission in ambient conditions (Fig. 1d), with a measured photoluminescence quantum yield (PLQY) of 10.03%, indicating the effect of gel on isolation oxygen. After extracted with dimethyl sulphoxide (DMSO), the cogel was collapsed and a solution contained Cu_5^- clusters was obtained, and then bubbled with nitrogen to isolate oxygen for the following experiments. To evaluate the influence of coassembly on the PL emission behaviour of Cu_5^- cluster, the emission spectra of Cu_5^- cluster in solution and cogel states were collected. As

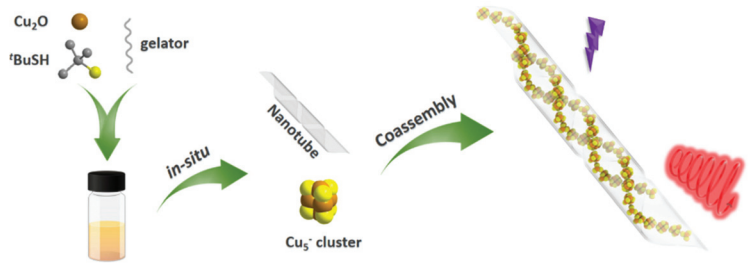

Scheme 1 Illustration of the coassembly of achiral Cu_5^- cluster and chiral gelator. Upon the excitation of UV-light, CPP could be obtained from the cogel.

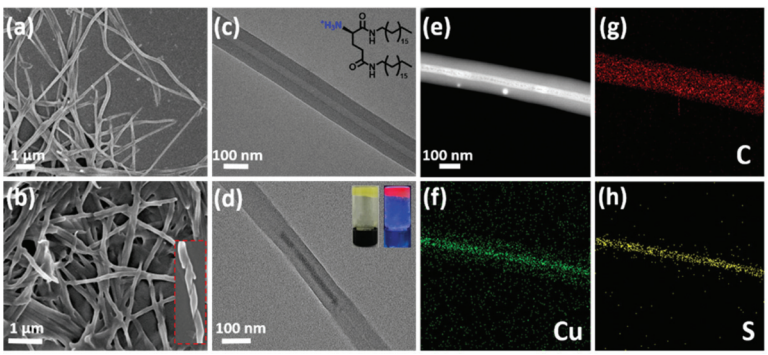

Fig. 1 SEM images of (a) D-G$^+$ gel and (b) D-G$^+$/Cu_5^- cogel. Inset of b: P-type helical nanotube of D-G$^+$/Cu_5^- cogel. TEM images of (c) D-G$^+$ gel and (d) D-G$^+$/Cu_5^- cogel. Inset of c: Molecular formula of the gelator D-G$^+$. Inset of d: Photo images of D-G$^+$/Cu_5^- cogel under day light (left) and UV irradiation (right). (e) HAADF-TEM image and (f–h) Cu, C and S elemental mapping of a strand of nanotube containing Cu_5^- clusters.

shown in Fig. S3,† the cogel exhibited similar spectrum compared with the Cu_5^- cluster in solution, implying the red emission of Cu_5^- cluster in cogel was retained. Moreover, the photoluminescence lifetimes of Cu_5^- cluster in solution and cogel states were investigated, and the microsecond lifetimes suggest the inherent phosphorescence. The lifetime of cogel is slightly longer than that of Cu_5^- cluster in solution (Fig. S4†), indicating the nonradiative decay of cluster was suppressed after coassembling. In addition, the identical wavelengths of electronic absorbance peaks between the Cu_5^- solution (Fig. S5†) and the reported Cu_5 clusters,[31] as well as the identical signals in electrospray ionization mass (ESI-MS) spectrum of the Cu_5^- solution demonstrate the structural stability of the Cu_5^- cluster during the coassembling process (Fig. S6†). It should be noted that the regular morphologies observed by TEM and SEM, and the emission spectrum further verified that the Cu_5^- clusters perfectly dispersed in the cogel without phase separation or individual aggregation.

Coassembly could dramatically improve the chiroptical properties compared with the individual building units. The chiral gelators D/L-G^+ show specific Cotton effect at 210 nm, while the Cu_5^- cluster is CD-silent in solution (Fig. S7†). After coassembling, the cogel shows a new Cotton effect at 310 nm, which is assigned to the absorption of Cu_5^- cluster, indicating the chirality transfer from the chiral gelator to Cu_5^- cluster. The fine mirror CD spectra of cogel, as well as the impressive g_{abs} value up to 0.018 for D-G^+/Cu_5^- cogel, are attributed to the fact that asymmetric packing orientation of Cu_5^- cluster is greatly enhanced by being confined in the chiral nanotubes (Fig. 2a and b). The g_{abs} value of the cogel is rather higher than that of chiral coassembled cocrystal[31] which is at the magnitude of 10^{-3} and larger than most of the chiral metal nanoclusters,[33] demonstrating that the supramolecular chirality induced by coassembly is beneficial to amplification of chiroptical asymmetry. The authenticity of the CD spectra obtained from the cogel systems could be confirmed by the linear dichroism (LD) measurement. The negligible linear dichroism compared with the CD spectrum of L-G^+/Cu_5^- cogel indicates that artefacts during the CD measurements can be excluded (Fig. S8†). Moreover, we also observed the mirror CPL spectra of the cogel with the g_{lum} value about 10^{-3}, comparing Cu_5^- cluster is CPP-silent (Fig. 2c, S9 and S10†). Inspired by this result and combining with the feature of the chiral gel, the supramolecular chiroptical switch of the cogel upon temperature was carried out. When the temperature was elevated to 80 °C, the cogel melted and the chirality transfer from chiral gelator to Cu_5^- cluster was blocked, leading to CPP silence. After cooling down to room temperature of 20 °C, the cogel regenerated and presented active CPP again. The chiroptical switch can be reversible for 5 cycles (Fig. 2d).

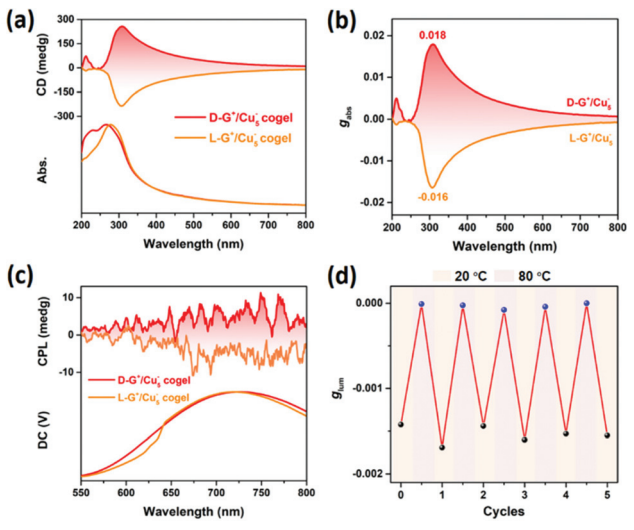

Fig. 2 (a) CD spectra of Cu_5^- clusters and gelators cogels. (b) g_{abs} values of the Cu_5^- clusters and gelators cogels. (c) CPL emission spectra of Cu_5^- clusters and gelators cogels. (d) g_{lum} values of the Cu_5^- clusters and gelators cogels at 20 °C and 80 °C.

To investigate the mechanism of chiral induction in cogel, CPL spectrum of disassembled mixture of Cu_5^- cluster and chiral gelator L-G^+ in chlorobenzene solution was tested. No obvious CPP signal was detected (Fig. S11†), indicating that the chirality transfer from the chiral gelator to Cu_5^- cluster is almost impossible in disassembled condition. As a comparison, a shorter chiral analogue named D-12G^+ was synthesized according to the literature.[9] After coassembling with Cu_5^- clusters, an incompact gel phase was formed following the same cogelation process of D-G^+/Cu_5^- cogel. Interestingly, only one weak Cotton effect at 231 nm was observed while no obvious signal was found at absorption region of Cu_5^- clusters (Fig. S12†), indicating that the chirality transfer from chiral D-12G^+ to Cu_5^- clusters was inhibited. Unlike the helical nanotubular morphology of the D-G^+/Cu_5^- cogel, D-12G^+/Cu_5^- cogel displayed lamellar structure without supramolecular chirality leading to loss of chiral induction (Fig. S13†). Compared with the CD-silent Cu_5^- cluster and weak Cotton effect of the chiral gelator at 210 nm, the cogel shows strong Cotton effect at the absorption area of Cu_5^- cluster (Fig. S7†), implying the chirality from the gelator transferring to Cu_5^- cluster during the coassembled process. The distribution of Cu_5^- clusters in the chiral nanotubes was observed under TEM investigation. Some places are filled tightly (like in Fig. 1d, e and S1†), while some are incompactly spread like in Fig. 3. To our delight, the Cu_5^- clusters were observed helically distributed along the nanotube in some places (Fig. 3). Helical nanoparticle superstructures directed by chiral templates have been investigated a lot,[34] yet helical cluster structures are very rare especially supported by chiral templates. According to the literature,[32] the formation mechanism of the nanotubular templates can be illustrated as shown in Fig. 3f. In ethanol solution, the nonpolar tail groups tend to form hydrophobic interactions with each other leading to the polar head groups to be outside to self-assemble into bilayers, and then to form intermediate plates to roll up into helical nanotubes due to chiral nature. The main driving forces are H-bond interactions among the head groups and hydrophobic interactions between the tail groups. The helical supramolecular structures formed spontaneously by chiral gelators can be reasonably considered to serve as templates for

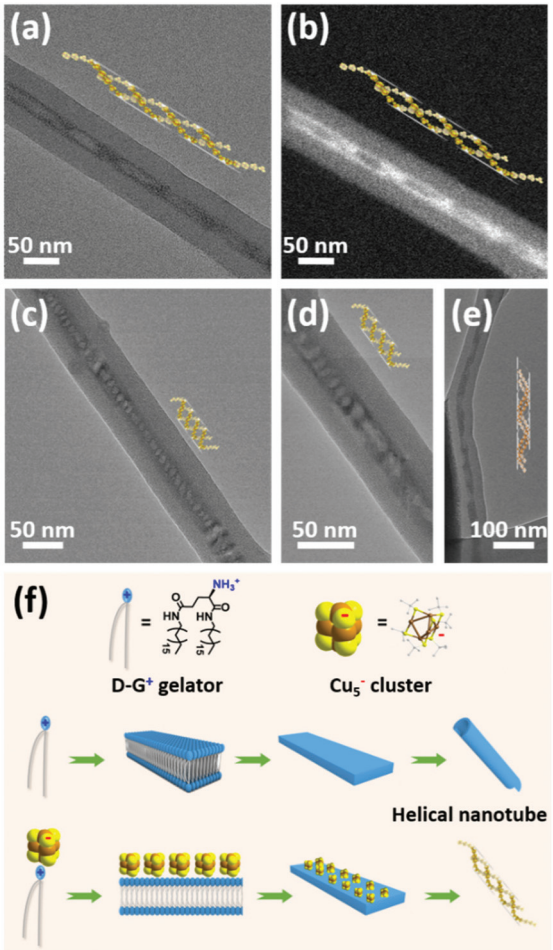

Fig. 3 (a, c and d) TEM images and (b) TEM dark field pattern image of D-G^+/Cu_5^- cogel. (e) TEM image of L-G^+/Cu_5^- cogel. Inset of images: Illustration of the helical distribution of the Cu_5^- clusters in nanotube. (f) Illustration of proposed mechanism for the formation of helical nanotube and helical arrangement of Cu_5^- clusters.

the helical cluster assemblies. The binding between the clusters and the helical nanotubes realized from the anionic Cu_5^- clusters and the protonated gelators, integrates with the confined effect of the nanotubes leading to the helical arrangement of the Cu_5^- clusters inside the nanotubes. It is noted that different helical morphologies of the Cu_5^- clusters are caused by different helical pitches, which depend on the rolling degree of the helical nanotubes. Therefore, the asymmetric arrangement of the clusters was along the growing direction of chiral nanotubes reflecting supramolecular chirality, which might be the primary reason for the induced chiroptical activities of the cogel system.

Conclusions

In conclusion, the supramolecular chirality and chiroptical properties of the achiral Cu_5^- cluster were successfully induced through helically confinined in the chiral gel, and the red phosphorescent emission of Cu_5^- cluster was lightened for the isolating oxygen of cogel. The Cu_5^- clusters were distributed along the assembled chiral nanotubes during the process of cogelation, achieving large Cotton effects with g_{abs} up to 0.018 and CPP emission. The asymmetric arrangement of the clusters along the chiral nanotubes plays an important role for the induced chiroptical activities. This work provides a facile and efficient approach for fabricating chiroptical assembled nanomaterials based on achiral coinage metal clusters which will be vigorously promoted for the application in constructing chiral functional materials. We further adopt this chiral assembled strategy on other coinage metal clusters for chirality generation and amplification. The universality of the strategy is proved and the relevant results will be displayed in the follow-up studies.

Conflicts of interest

There are no conflicts to declare.

Acknowledgements

This work was financially supported by the National Natural Science Foundation of China (No. 21975065, 92061201, U21A20277, 21825106) and Zhengzhou University.

Notes and references

1 M. Liu, L. Zhang and T. Wang, Supramolecular chirality in self-assembled systems, *Chem. Rev.*, 2015, **115**, 7304–7397.
2 P. Xing and Y. Zhao, Controlling supramolecular chirality in multicomponent self-assembled systems, *Acc. Chem. Res.*, 2018, **51**, 2324–2334.
3 L. Zhang, L. Qin, X. Wang, H. Cao and M. Liu, Supramolecular chirality in self-assembled soft materials: regulation of chiral nanostructures and chiral functions, *Adv. Mater.*, 2014, **26**, 6959–6964.
4 S. Huang, H. Yu and Q. Li, Supramolecular chirality transfer toward chiral aggregation: asymmetric hierarchical self-assembly, *Adv. Sci.*, 2021, **8**, 2002132.
5 T. Wen, H.-F. Wang, M.-C. Li and R.-M. Ho, Homochiral evolution in self-assembled chiral polymers and block copolymers, *Acc. Chem. Res.*, 2017, **50**, 1011–1021.
6 E. Yashima, N. Ousaka, D. Taura, K. Shimomura, T. Ikai and K. Maeda, Supramolecular helical systems: helical assemblies of small molecules, foldamers, and polymers with chiral amplification and their functions, *Chem. Rev.*, 2016, **116**, 13752–13990.
7 G. Albano, G. Pescitelli and L. Di Bari, Chiroptical properties in thin films of π-conjugated systems, *Chem. Rev.*, 2020, **120**, 10145–10243.
8 J. L. Greenfield, J. Wade, J. R. Brandt, X. Shi, T. J. Penfold and M. J. Fuchter, Pathways to increase the dissymmetry in the interaction of chiral light and chiral molecules, *Chem. Sci.*, 2021, **12**, 8589–8602.

9 T. Goto, Y. Okazaki, M. Ueki, Y. Kuwahara, M. Takafuji, R. Oda and H. Ihara, Induction of strong and tunable circularly polarized luminescence of nonchiral, nonmetal, low-molecular-weight fluorophores using chiral nanotemplates, *Angew. Chem., Int. Ed.*, 2017, **56**, 2989–2993.
10 J. Han, J. You, X. Li, P. Duan and M. Liu, Full-color tunable circularly polarized luminescent nanoassemblies of achiral AIEgens in confined chiral nanotubes, *Adv. Mater.*, 2017, **29**, 1606503.
11 S. Huo, P. Duan, T. Jiao, Q. Peng and M. Liu, Self-assembled luminescent quantum dots to generate full-color and white circularly polarized light, *Angew. Chem., Int. Ed.*, 2017, **56**, 12174–12178.
12 Y. Shi, P. Duan, S. Huo, Y. Li and M. Liu, Endowing perovskite nanocrystals with circularly polarized luminescence, *Adv. Mater.*, 2018, **30**, 1705011.
13 X. Jin, Y. Sang, Y. Shi, Y. Li, X. Zhu, P. Duan and M. Liu, Optically active upconverting nanoparticles with induced circularly polarized luminescence and enantioselectively triggered photopolymerization, *ACS Nano*, 2019, **13**, 2804–2811.
14 M. Zhou, Y. Sang, X. Jin, S. Chen, J. Guo, P. Duan and M. Liu, Steering nanohelix and upconverted circularly polarized luminescence by using completely achiral components, *ACS Nano*, 2021, **15**, 2753–2761.
15 X. Kang and M. Zhu, Tailoring the photoluminescence of atomically precise nanoclusters, *Chem. Soc. Rev.*, 2019, **48**, 2422–2457.
16 N. Goswami, Q. Yao, Z. Luo, J. Li, T. Chen and J. Xie, Luminescent metal nanoclusters with aggregation-induced emission, *J. Phys. Chem. Lett.*, 2016, **7**, 962–975.
17 S. Takano and T. Tsukuda, Amplification of the optical activity of gold clusters by the proximity of BINAP, *J. Phys. Chem. Lett.*, 2016, **7**, 4509–4513.
18 M. Zhu, H. Qian, X. Meng, S. Jin, Z. Wu and R. Jin, Chiral Au25 nanospheres and nanorods: synthesis and insight into the origin of chirality, *Nano Lett.*, 2011, **11**, 3963–3969.
19 Q. Xu, S. Kumar, S. Jin, H. Qian, M. Zhu and R. Jin, Chiral 38-gold-atom nanoclusters: synthesis and chiroptical properties, *Small*, 2014, **10**, 1008–1014.
20 J.-Q. Wang, Z.-J. Guan, W.-D. Liu, Y. Yang and Q.-M. Wang, Chiroptical activity enhancement via structural control: the chiral synthesis and reversible interconversion of two intrinsically chiral gold nanoclusters, *J. Am. Chem. Soc.*, 2019, **141**, 2384–2390.
21 G. Deng, S. Malola, J. Yan, Y. Han, P. Yuan, C. Zhao, X. Yuan, S. Lin, Z. Tang, B. K. Teo, H. Häkkinen and N. Zheng, From symmetry breaking to unraveling the origin of the chirality of ligated Au13Cu2 Nanoclusters, *Angew. Chem., Int. Ed.*, 2018, **57**, 3421–3425.
22 M. Sugiuchi, Y. Shichibu and K. Konishi, An inherently chiral Au24 framework with double-helical hexagold strands, *Angew. Chem., Int. Ed.*, 2018, **57**, 7855–7859.
23 H. Yoshida, M. Ehara, U. D. Priyakumar, T. Kawai and T. Nakashima, Enantioseparation and chiral induction in Ag29 nanoclusters with intrinsic chirality, *Chem. Sci.*, 2020, **11**, 2394–2400.
24 S. Knoppe, O. A. Wong, S. Malola, H. Häkkinen, T. Bürgi, T. Verbiest and C. J. Ackerson, Chiral phase transfer and enantioenrichment of thiolate-protected Au102 Clusters, *J. Am. Chem. Soc.*, 2014, **136**, 4129–4132.
25 Z. Wu, Q. Yao, S. Zang and J. Xie, Directed Self-Assembly of Ultrasmall Metal Nanoclusters, *ACS Mater. Lett.*, 2019, **1**, 237–248.
26 Z. Xie, P. Sun, Z. Wang, H. Li, L. Yu, D. Sun, M. Chen, Y. Bi, X. Xin and J. Hao, Metal–organic gels from silver nanoclusters with aggregation-induced emission and fluorescence-to-phosphorescence switching, *Angew. Chem., Int. Ed.*, 2020, **59**, 9922–9927.
27 H. Wu, X. He, B. Yang, C.-C. Li and L. Zhao, Assembly-induced strong circularly polarized luminescence of spirocyclic chiral silver(I) clusters, *Angew. Chem., Int. Ed.*, 2021, **60**, 1535–1539.
28 L. Shi, L. Zhu, J. Guo, L. Zhang, Y. Shi, Y. Zhang, K. Hou, Y. Zheng, Y. Zhu, J. Lv, S. Liu and Z. Tang, Self-assembly of chiral gold clusters into crystalline nanocubes of exceptional optical activity, *Angew. Chem., Int. Ed.*, 2017, **56**, 15397–15401.
29 Z. Wu, Y. Du, J. Liu, Q. Yao, T. Chen, Y. Cao, H. Zhang and J. Xie, Aurophilic interactions in the self-assembly of gold nanoclusters into nanoribbons with enhanced luminescence, *Angew. Chem., Int. Ed.*, 2019, **58**, 8139–8144.
30 C. Zhang, S. Li, X.-Y. Dong and S.-Q. Zang, Circularly polarized luminescence of agglomerate emitters, *Aggregate*, 2021, **2**, e48.
31 Y. Jin, S. Li, Z. Han, B.-J. Yan, H.-Y. Li, X.-Y. Dong and S.-Q. Zang, Cations controlling the chiral assembly of luminescent atomically precise copper(I) clusters, *Angew. Chem., Int. Ed.*, 2019, **58**, 12143–12148.
32 X. Zhu, Y. Li, P. Duan and M. Liu, Self-assembled ultralong chiral nanotubes and tuning of their chirality through the mixing of enantiomeric components, *Chem. – Eur. J.*, 2010, **16**, 8034–8040.
33 Y. Zhu, J. Guo, X. Qiu, S. Zhao and Z. Tang, Optical activity of chiral metal nanoclusters, *Acc. Mater. Res.*, 2021, **2**, 21–35.
34 S. Mokashi-Punekar, Y. Zhou, S. C. Brooks and N. L. Rosi, Construction of chiral, helical nanoparticle superstructures: progress and prospects, *Adv. Mater.*, 2020, **32**, 1905975.

